



Karbala International Journal of Modern Science

Manuscript 3314

Synthesizing of Alginate Coated-Silver Nanoparticles Core-Shell for Detecting of S-naproxen Enantiomer in Pharmaceutical Formulation

Abdolrasol Barazandeh

Ghasem Najafpour-Darz

Afshar Alihossein

Sohrab Kazemi

Follow this and additional works at: <https://kijoms.uokerbala.edu.iq/home>

 Part of the [Biology Commons](#), [Chemistry Commons](#), [Computer Sciences Commons](#), and the [Physics Commons](#)

Synthesizing of Alginate Coated-Silver Nanoparticles Core-Shell for Detecting of S-naproxen Enantiomer in Pharmaceutical Formulation

Abstract

Core-shell nanoparticles were used in a unique direct UV-Vis spectrophotometric technique to detect the S-naproxen enantiomer. Silver nanoparticles (Ag NPs) covered with sodium alginate (Alg) shell, a naturally occurring biopolymer, made the core of the nanostructure. To name a few, TEM, FESEM, UV-Visible, DLS, ZP, AFM, XRD, EDX and FT-IR are among the analytical methods used to analyze the creation of the core-shell structure. Based on obtained results, spherical Ag@ Alg NPs with an average size of 27.4 nm (DTEM), hydrolytic size of 46 nm (DDLs) and surface charge of -60.9 mV were successfully synthesized. The effect of various reaction time and pH values on determining the s-naproxen enantiomer by Ag@ Alg NPs was investigated. Determining the maximum S-naproxen enantiomer was at a reaction time of 8 min and pH 8. According to the international council for the harmonization of technical requirements for pharmaceuticals for human use (ICH) guidelines, the detection limit and quantitative limit of S-naproxen enantiomer were determined to be 1.87×10^{-4} mol/L and 5.64×10^{-4} mol /L. This clearly indicates that the alginate-coated silver nanoparticle

Keywords

alginate; Core-shell nanoparticles; Green chemistry; S-Naproxen; Silver nanoparticles; UV-Vis, spectrophotometric

Creative Commons License



This work is licensed under a [Creative Commons Attribution-Noncommercial-No Derivative Works 4.0 License](https://creativecommons.org/licenses/by-nc-nd/4.0/).

RESEARCH PAPER

Synthesizing of Alginate Coated-silver Nanoparticles Core-shell for Detecting of S-naproxen Enantiomer in Pharmaceutical Formulation

Abdolrasol Barazandeh ^a, Ghasem Najafpour-Darzi ^b,
Afshar Alihosseini ^{a,*}, Sohrab Kazemi ^c

^a Department of Chemical Engineering Central Tehran Branch, Islamic Azad University, Tehran, Iran

^b Faculty of Chemical Engineering, Babol Noshirvani University of Technology, Babol, Iran

^c Department of Pharmacology and Physiology, School of Medicine, Babol University of Medical Sciences, Babol, Iran

Abstract

Core-shell nanoparticles were used in a unique direct UV–Vis spectrophotometric technique to detect the S-naproxen enantiomer. Silver nanoparticles (Ag NPs) covered with sodium alginate (Alg) shell, a naturally occurring biopolymer, made the core of the nanostructure. To name a few, TEM, FESEM, UV–Visible, DLS, ZP, AFM, XRD, EDX and FT-IR are among the analytical methods used to analyze the creation of the core–shell structure. Based on obtained results, spherical Ag@ Alg NPs with an average size of 27.4 nm (DTEM), hydrolytic size of 46 nm (DDLS) and surface charge of –60.9 mV were successfully synthesized. The effect of various reaction time and pH values on determining the s-naproxen enantiomer by Ag@ Alg NPs was investigated. Determining the maximum S-naproxen enantiomer was at a reaction time of 8 min and pH 8. According to the international council for the harmonization of technical requirements for pharmaceuticals for human use (ICH) guidelines, the detection limit and quantitative limit of S-naproxen enantiomer were determined to be 1.87×10^{-4} mol/L and 5.64×10^{-4} mol/L. This clearly indicates that the alginate-coated silver nanoparticle core–shell can be used to measure S-naproxen enantiomer through green chemistry without using toxic chemicals.

Keywords: Alginate, S-Naproxen, Silver nanoparticles, UV–vis spectrophotometry

1. Introduction

Regarding IUPAC, naproxen d-2-(6-methoxy-2naphthyl) propionic acid, often known as naproxen, is a non-steroidal anti-inflammatory medicine having with a number of medicinal uses including analgesic, antipyretic, and anti-inflammatory drugs [1,2]. The chiral carbon atom in naproxen holds two enantiomers, S-naproxen and R-naproxen. S-naproxen is one of them which has pharmaceutical uses in curing illnesses [3]. Indicators for assessing the quality of chiral pharmaceuticals have been established in accordance with the guidelines provided by the International Conference on Harmonization of Technical

Requirements for the Registration of Drugs for Human Use (ICH) [4]. This guideline suggests that the inactive enantiomer in the drug is an impurity. Furthermore, it is essential to develop tests that are able to detect the enantiomers. It is necessary to provide effective quality control tools to ensure proper and safe production [5]. In fact, the impurities created in the drug that may be created in different stages of development, transportation, and storage should be identified and measured in the drug. The types of common analytical techniques used in drug analysis include titrimetric, chromatography, Raman spectroscopy, electrophoretic and electrochemical. Analytical tools and methods play an important role in identifying and measuring the

Received 5 April 2023; revised 6 July 2023; accepted 8 July 2023.
Available online 21 September 2023

* Corresponding author.
E-mail address: afshar.alihosseini@gmail.com (A. Alihosseini).

<https://doi.org/10.33640/2405-609X.3314>

2405-609X/© 2023 University of Kerbala. This is an open access article under the CC-BY-NC-ND license (<http://creativecommons.org/licenses/by-nc-nd/4.0/>).

drug. In this context, spectrophotometry is a well-known fast and low cost analytical method for determining the drugs [6,7]. These components must be made while embracing the adaptable criteria as listed below. Due to its speed, accessibility, and ease of use, ultraviolet–visible spectrophotometry (UV–Vis) is a frequently employed analytical technique in scientific study. Due to the development of this technology, UV–vis spectrometry is now extensively utilized as a straightforward, sensitive, trustworthy and affordable method that enables determining the extremely low quantities of chemicals and using very tiny sample sizes. It also provides adaptability and mobility of the tools and created approaches, which have been also a great contribution to the long-term usage of UV–vis spectroscopy. Using this analytical technique subjects to generate no residues when using solvents. So far, various chemicals were detected using UV–Vis spectrophotometry method such as nucleic acids, amino acids, carbohydrates and protein [8,9]. Although this method was extensively used to detect Naproxen, their reagent was mostly toxic chemicals [10,11]. Considering the unique physico-chemical properties of metal nanoparticles and their wide range of applications including biomedical and catalytic activities, they have the chemical replacement potential [12,13]. Combining UV–Vis spectrophotometric method with nanotechnology using metal nanoparticles based on their small size and high surface area could be an efficient approach to improve the performance of system detecting low concentration of the desired molecules [14,15]. Since Ag NPs have strong surface Plasmon resonance (SPR), they can be used to detect different organic and mineral compounds using a spectrophotometer [16,17]. It is indicated that selecting an appropriate stabilizer for Ag NPs plays a critical role for the selectivity and sensitivity of Ag-based nanostructures [10–18]. So far, various biopolymers like gelatin, chitosan, starch, alginate and cellulose were used for the surface modification of Ag [19,20]. Hence, spectrophotometric method was practiced to scrutinize the enantiomers of tryptophan using chitosan-capped silver nanoparticles [6]. Furthermore, in another study, starch-coated silver nanoparticles were used to detect naproxen. Silver nanoparticles with starch coating, citrate coating and bare silver nanoparticles all differently responded to R- and S-naproxen. Based on the results of that study, bare Ag NPs and citrate-containing silver cannot detect R- and S-Naproxen, whereas silver nanoparticles with starch coating are able to detect them [15]. Yet, no serious research has been carried out to determine S-naproxen

enantiomer using silver nanoparticles coated with alginate (Ag@Alg NPs). For the first time, core–shell nanoparticles were used to identify S-enantiomer of naproxen through green chemistry without using toxic chemical solvents in direct UV–Vis spectroscopic technique. The core and shell of nanostructure is composed of silver nanoparticles (Ag NPs) and alginate (Alg), respectively. The novelty of this work is to evaluate the relationship between reaction time and pH to detect the UV–Vis spectrophotometry of S- naproxen enantiomer using core–shell metal NPs.

2. Material and methods

2.1. Material

Sodium borohydride (NaBH_4), sodium alginate ($\text{C}_6\text{H}_9\text{NaO}_7$), sodium hydroxide (Na OH), sodium citrate ($\text{C}_6\text{H}_5\text{Na}_3\text{O}_7$) and silver nitrate (AgNO_3) were purchased from Sigma–Aldrich Company (St. Louis, Mo, USA). S- Naproxen was supplied by Tehran Daru Company (Tehran, Iran). Deionized water was used throughout the experiments. The phosphate buffer was used for pH range of 4–10.

2.2. Methods

2.2.1. Synthesis of Ag@ Alg NPs

Silver NPs coated with alginate (Ag@ Alg NPs) were synthesized based on a developed method reported in literature [21]. 50 mL of sodium alginate (1.5%) was added to 50 mL of an aqueous solution of silver nitrate (0.05 m M) to prepare a mixture of silver nitrate with alginate polysaccharide. Then, the pH of the prepared solution was adjusted to 11.7 using 1 M Na OH solution. The prepared solution was stirred by a magnetic stirrer at 60 °C for 15 min. Finally, the concentration of silver NPs capped by alginate was calculated using the extinction coefficient of Ag NPs and Beer's law [15]. In fact, the alginate acts as a stabilizer; assisted the method to be a powerful technique as a green synthetic approach for the synthesis of Ag-NPs. Na OH solution (alkaline pH) is the main reducing agent in the Ag seed (Ag°) capped by Alginate. For analytical application, the produced alginate-coated silver nanoparticles were kept at room temperature.

2.2.2. Preparation of S- naproxen samples and calibration curve

The pure S-naproxen sample (50 mg) was dissolved in 50 mL of methanol. The prepared sample was diluted up to 100 mL using methanol as solvent. The calibration plot was prepared using the above

S-naproxen sample solutions at concentrations ranging from 0.1 to 1 μ mol/ml. The absorption of naproxen was recorded using UV–Vis spectroscopy at the wavelength of 272 nm. In the S-naproxen absorption calibration plot, the linear relation was determined using linear least squares regression.

2.2.3. Characterization of Ag@ Alg NPs

The following analytical tools were used to characterize the Ag@ Alg NPs: transmission electron microscope (TEM, Zeiss EM900 model), scanning electron microscope (SEM, TESCAN-Mira 3Lmu, model), Fourier transform infrared spectroscopy (FT-IR, Thermo Scientific Nicolet 8700 model), UV–Vis spectroscopy (Perkin Elmer Lambda UV–Vis 950 spectrophotometer), dynamic light-s (Perkin Elmer, model, USA).

2.2.4. Optimal reaction time and pH for detection of S-naproxen with Ag@ Alg NPs

Finding the minimum reaction time for new Ag @ Alg NPs reagent in the clinical laboratory is an essential parameter. In order to develop a new Ag @ Alg NPs reagent, it is important that the reaction between naproxen and Ag @Alg nanoparticles reaches a stable condition in a minimum time, and remains constant as time drags on. For this purpose, the effect of reaction time among silver nanoparticles with coating the Alginate and naproxen on the absorption of S-naproxen within 1–12 min was investigated. As silver nanoparticles in a pH < 3 are not stable, buffers in the pH range of 4.0–10.0 have been used to analyze the effects of pH values on the absorption process.

3. Results and discussion

3.1. Characterization of Ag@ Alg NPs

To detect naproxen by UV–Vis spectrophotometry, alginate was grafted onto Ag nanostructures via bidentate bridging to form a biodegradable polymer. A schematic illustration of alginate loaded on Ag NPs is illustrated in Fig. 1. The results of various characterizations of Ag@ Alg NPs are presented in this section.

3.1.1. Results of UV–vis-spectroscopy and XRD analyzes

UV–visible absorption spectra of Ag@ Alg NPs, silver nitrate and sodium alginate in the range of 200–700 nm are displayed in Fig. 2. No significant absorption peaks were observed in the investigated wavelength in the sodium alginate curve in Fig. 2 (red line). A strong peak and broader appeared in the

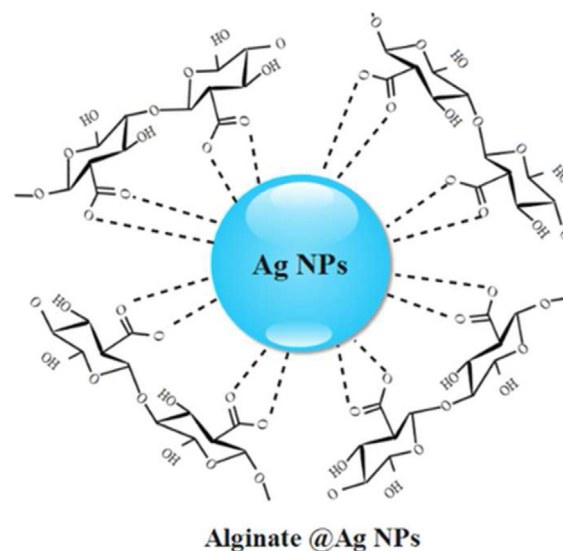


Fig. 1. A Schematic illustration of the alginate Functionalized-Ag NPs.

UV–Vis spectrum of Ag@ Alg NPs at 415 nm, indicates silver nanoparticles Fig. 2 (black curve), and validates the formation of Ag-based NPs [21]. The XRD pattern of Ag@ Alg NPs s is shown in Fig. 3. The peaks situated at 38.23°, 44.30°, 64.58° and 77.45° ascribed to the diffraction planes of cube silver (111, 200, 220, 311) [22,23]. No extra peak attributed to the impurity can be observed in XRD spectrum Ag@ Alg NPs. As a result, this confirms the formation of pure silver based-NPs with crystalline structure.

3.1.2. Results of TEM, SEM, and AFM analyses

The size, and morphology Ag@ Alg NPs were characterized using TEM analysis. TEM image of Ag@ Alg NPs (Fig. 4a) indicates the formation of spherical NPs. Moreover, the average size of alginate-coated silver nanoparticles was 27.4 nm and

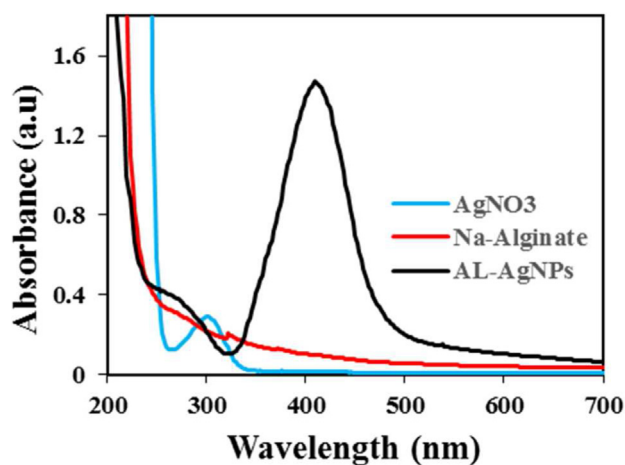


Fig. 2. UV–Visible spectrum of sodium alginate (red curve), silver nitrate (blue curve), and Ag@ Alg NPs (black curve).

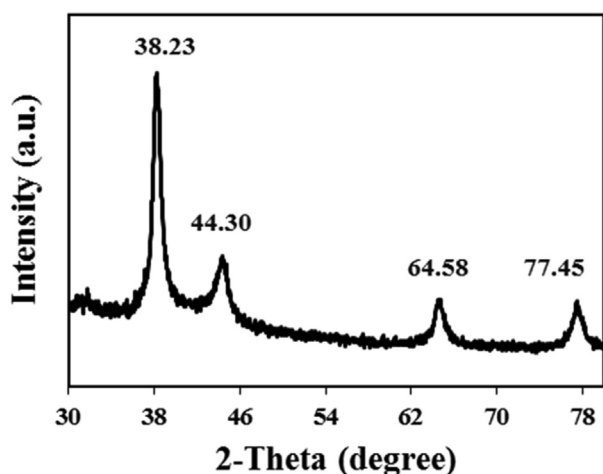


Fig. 3. X-ray diffraction pattern of Ag@ Alg NPs.

the TEM image of alginate-coated silver nanoparticles was calculated using 35 independent nanoparticles by Image J software (Fig. 4b).

To further study the size and morphology of Ag@ Alg NPs, AFM analysis was performed. Based on the

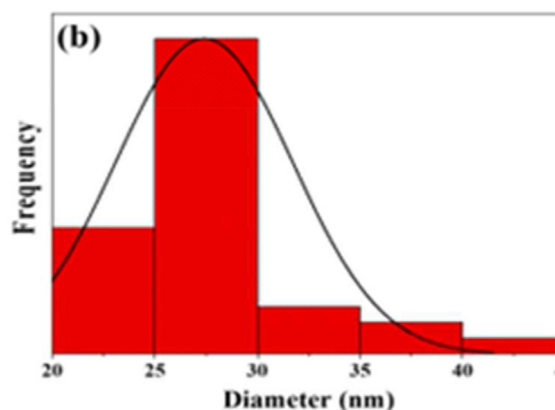
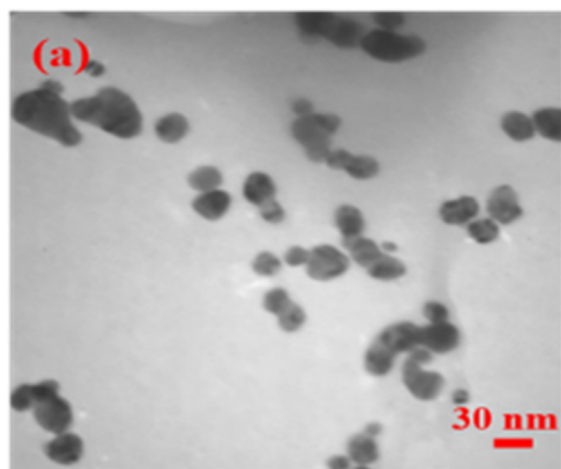


Fig. 4. TEM image (a) and size distribution (b).

results of AFM (Fig. 5a and b), Ag@ Alg NPs are spherical with the average size of 29 nm (Fig. 5c), validating the result of NPs size obtained by TEM analysis. The results of SEM analysis of Ag@ Alg NPs at magnification of 135 Kx are shown in Fig. 6. Moreover, it is concluded that from this figure it is clear that the synthesized Ag@ Alg NPs were spherical and formed small aggregates [24].

3.1.3. Results of DLS and zeta potential analyzes

The results of DLS of Ag @Alg nanoparticles at two different pH values are presented in Fig. 7. Based on this analysis, the average hydrodynamic diameter of Ag @Alg nanoparticles for pH 7 and 10 was 82.6 nm (PDI: 0.4) and 107 nm (PDI: 0.599) for pH values 7 and 10, respectively. These values indicated that the structure of Ag @Ag nanoparticles at pH 7 is more stable than at pH 10. The result of zeta potential analysis of Ag@ Alg NPs is indicated in Fig. 8. Ag@ Alg NPs were found to have a mean surface charge of -60.9 mV at pH 7, which suggests that the highly negative charge core-shell NPs were formed. According to the American Society for Testing and Materials (ASTM), moderate stability can be indicated for the stability of NPs suspension if the value of Zeta potential is between 30 and 40 mV, either positive or negative. On the other hand, the zeta potential value more than 40 mV refers to the high stable NPs suspension [25]. Therefore, based on DLS and zeta potential analyzes, it can be concluded that the synthesized Ag@ Alg NPs possess desirable stability at neutral pH. As a result, NPs are suitable for analytical applications without any additional buffer.

3.1.4. Results of FT-IR analyses

FT-IR analysis was performed to determine the functional groups of Ag@ Alg NPs. Fig. 9 (red) displays the FT-IR spectrum of sodium alginate comprising the broad peak of OH groups at 3500 cm^{-1} , characteristic peaks at 2927 cm^{-1} and 2355 cm^{-1} attributed to the carbonyl functional groups and the peak at 1639 cm^{-1} related to stretching of C=C alkene groups. The peak positioned at 1405 cm^{-1} is related to C-O vibration of the alginate backbone [26,27]. The same peaks appeared in the FT-IR spectrum of Ag@ Alg NP, validating the formation of core-shell nanostructure using alginate polymer (Fig. 9 (black)). In comparison with the FT-IR spectrum of sodium alginate (Fig. 9 (red)), the intensity of peaks at 3473 cm^{-1} and 1600 cm^{-1} increased in the spectrum of Ag@ Alg NPs (Fig. 9 (black)), which could be on account of the participation of carboxyl groups (COOH) and hydroxyl groups (OH) in the conjugation of alginate on the surface of silver NPs. Validating the formation of

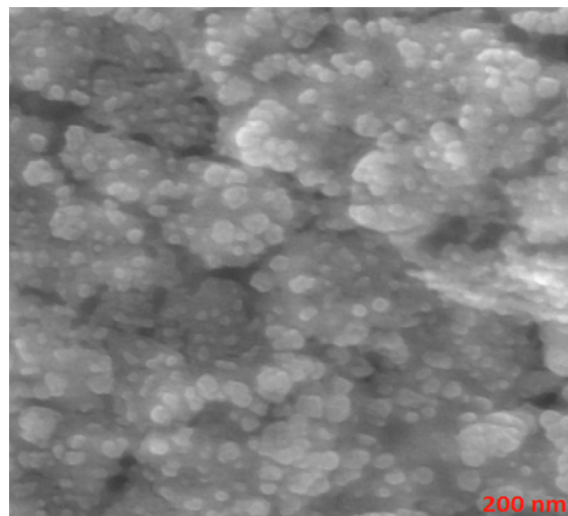
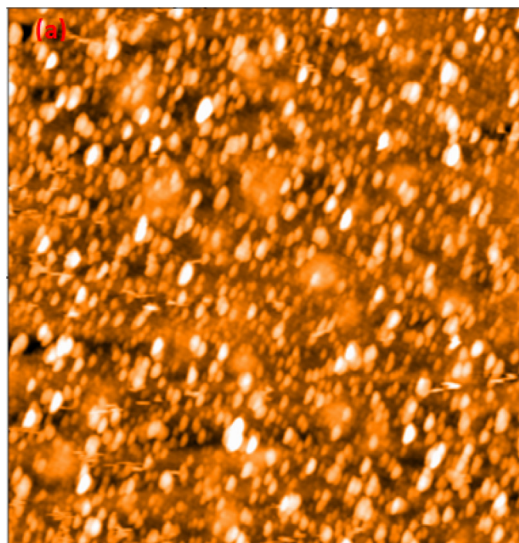


Fig. 6. SEM image.

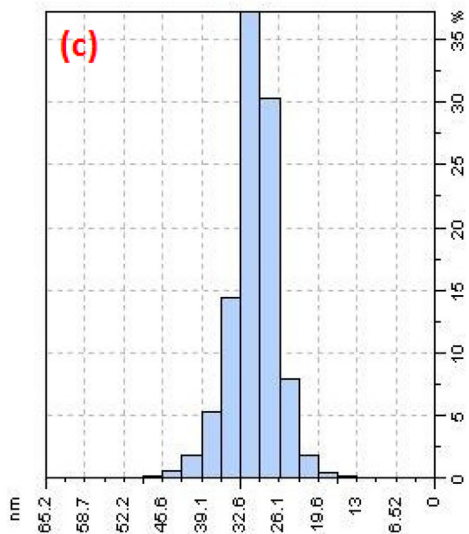
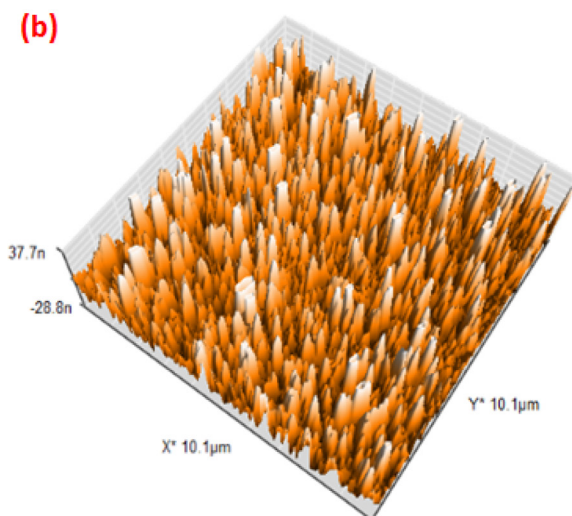


Fig. 5. AFM surface topography(a) & (b) and (c) size distribution of Ag@ Alg NPs using AFM analysis.

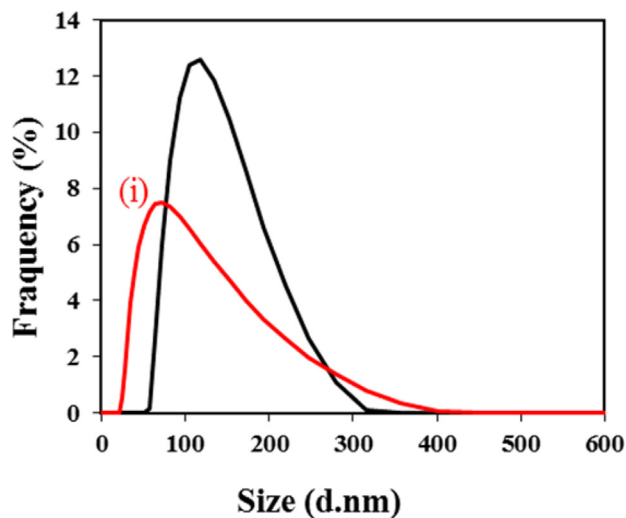


Fig. 7. Hydrodynamic diameter of Ag@ Alg NPs at two pH values of 7 (red) and 10 (black).

core-shell nanostructure using alginate polymer. Compare to FT-IR spectrum of sodium alginate (Fig. 9 (red)), the intensity of peaks at 3473 cm^{-1} and 1600 cm^{-1} increased in the spectrum of Ag@ Alg NPs (Fig. 9 (black)), which could be attributed to the participation of carboxyl groups (COOH) and hydroxyl groups (OH) in the conjugation of alginate on the surface of silver NPs.

3.1.5. Results of EDX analyses

Energy-dispersive X-ray analysis (EDX) was used to evaluate the chemical composition of the silver nanoparticles coated with alginate. The presence of peaks related to Ag, Na and O elements in silver

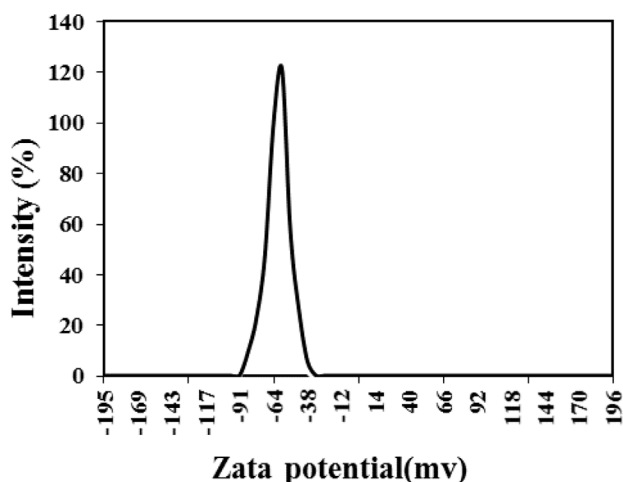


Fig. 8. Zeta potential of Ag@ Alg NPs at pH 7.

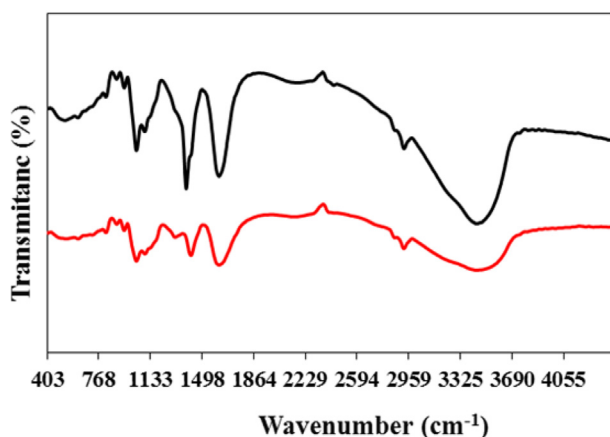


Fig. 9. FT-IR spectra of sodium alginate (red) and Ag@ Alg NPs (black).

nanoparticles (NPs Ag) coated with sodium alginate (Alg) is shown in Fig. 10.

3.2. Naproxen detection using Ag@ Alg NPs

3.2.1. Results of UV–Vis spectroscopy

Fig. 11 illustrates the UV–Vis spectra of pure S-naproxen and mixture of S-naproxen and Ag@ Alg NPs. Compared with the mixture of S-naproxen and Ag@ Alg NPs (Fig. 11 (black)), no absorption peak can be detected in the UV–Vis spectrum of pure S-naproxen at the wavelength of 414 nm (Fig. 11 (red)). Furthermore, a peak at 272 nm can be observed in the spectrum of pure S-naproxen (Fig. 11 (red)), which was appeared in the UV–Vis spectrum of mixture of S-naproxen and Ag@ Alg NPs (Fig. 11 (black)). Consequently, UV-VIS spectrophotometers can detect S-naproxen using Ag@ Alg NPs at 272 nm. Fig. 12 shows the detection of S-naproxen in the concentration range of

0.1–1 $\mu\text{mol/mL}$ with Ag@ Alg NPs at the wavelength of 272 nm using UV–Vis spectrophotometer. Based on our experimental results, it was indicated that the empty silver nanoparticles couldn't detect S-naproxen in the range of 0.1–1 $\mu\text{mol/mL}$, nevertheless silver nanoparticles with alginate coating could detect naproxen.

3.2.2. Results of calibration curve

As shown in Fig. 13, under the optimum condition, the absorption spectra of Alg @ Ag NPs were recorded in the presence of different amounts of S-naproxen enantiomer. The calibration curve for the S-naproxen enantiomer under optimal conditions, with a correlation coefficient of 0.993 in the concentration range of 0.1–1 $\mu\text{mol/mL}$ was linear.

3.2.3. Effect of reaction time and pH on S-naproxen detection

The results of the pH reaction on the detection of S-naproxen were presented in Fig. 14. In this research, it was concluded that the detection of S-naproxen using Ag@ Alg NPs was low at acidic pH levels because NP precipitation occurred at low pH. In fact, it reduces the contact area between S-naproxen and the Ag@ Alg NPs. As observed in Fig. 14, the absorption of S-naproxen increased at pH 8 as the pH of the solution was raised (by adding 0.1 M NaOH solution). Meanwhile, the absorption of S-naproxen decreased at high alkaline conditions. It could be explained by the repulsion force between S-naproxen molecules at high pH values subjected to a low interaction between the drug and the surface of Ag@ Alg NPs. The effect of reaction time in the range of 1–12 min on the detection of S-naproxen using Ag@ Alg NPs was investigated. As shown in Fig. 15, the absorption of S-naproxen was approximately constant within 2 min, then increased up to 4 min, and the maximum absorption was observed for 8 min. After that, increasing the reaction time

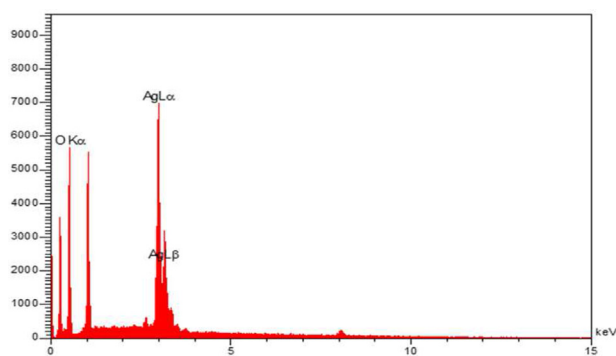


Fig. 10. EDX spectrum.

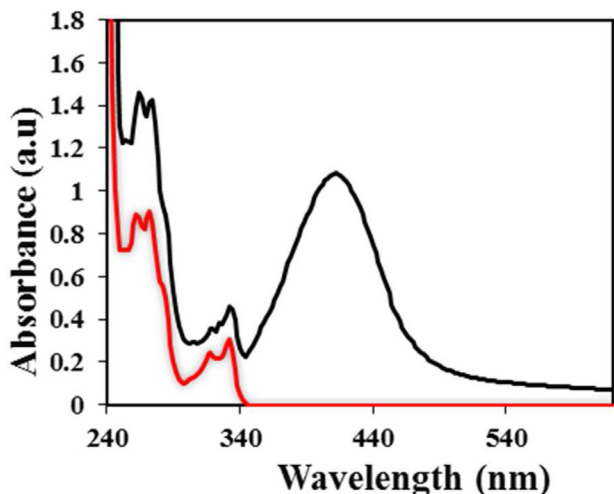


Fig. 11. UV–Vis spectra of pure naproxen (red) and combination of naproxen and Ag@ Alg NPs (black).

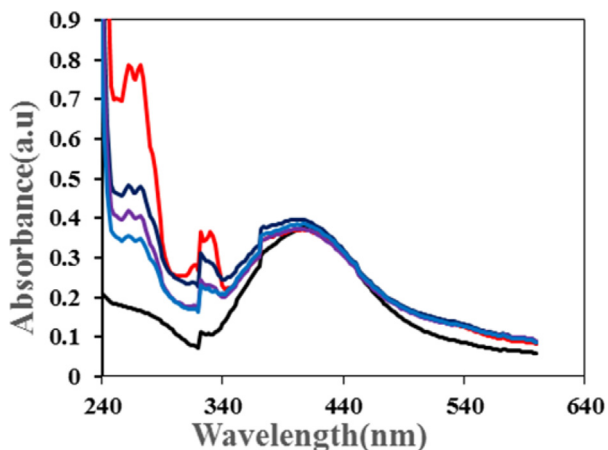


Fig. 12. UV–Vis spectra pure Ag@ Alg NPs (black color) and combination of naproxen concentration range of 0.1–1 μmolL^{-1} and Ag@ Alg NPs.

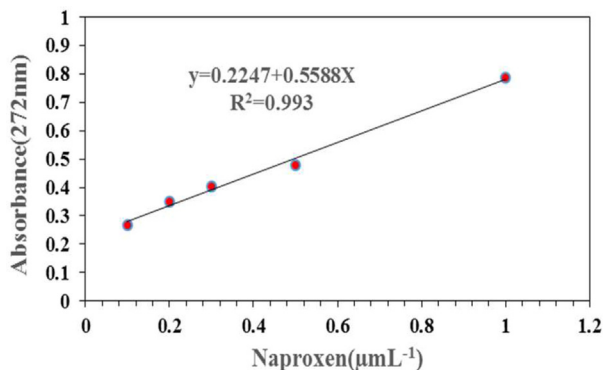


Fig. 13. Calibration plot of naproxen loaded on Alg @ Ag NPs.

had negative effect on the detection of S-naproxen. So, the reaction time of 8 min was considered as the desired time for S-naproxen detection. The rest of experimental were conducted at the modified reaction time of 8 min.

3.2.4. Determination of naproxen

Different naproxen concentrations were found and analyzed using coated-silver nanoparticles core–shell as a reagent by a spectrophotometer with variations of 20 μg per liter and an estimated relative error of 1%. The obtained results and recovery values are summarized in Table 1.

3.3. Validation method

According to the International Union of Pure and Applied Chemistry (IUPAC), the limit of detection

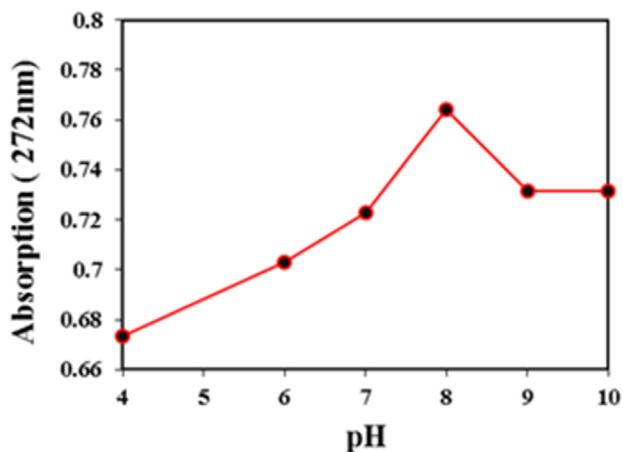


Fig. 14. Effect of reaction time on the detection of naproxen using Ag@ Alg NPs.

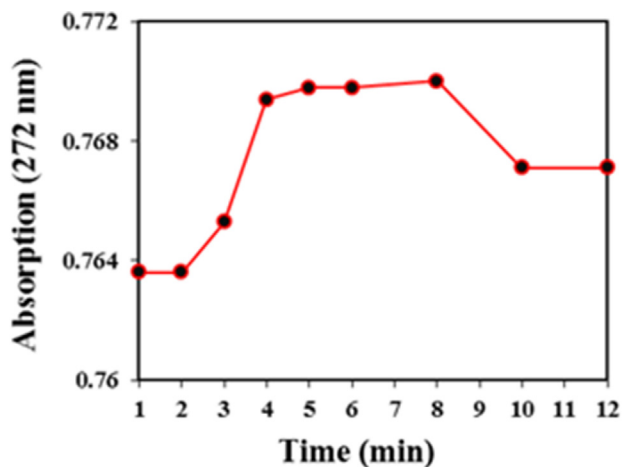


Fig. 15. Effect of solution pH on the detection of naproxen using Ag@ Alg NPs.

(LOD) is the smallest amount of analyte required to produce a signal that can be discriminated from a blank sample in terms of magnitude [29]. The lowest concentration of analyte at which analyte can be measured is known as the limit of quantification (LOQ) [30]. Considering the importance of LOD and LOQ parameters for the validation of an analytical method; we further measured the values of these two parameters. Based on the international council for the harmonization of technical requirements for pharmaceuticals for human use (ICH) guidelines, the equations of $LOD = 3.3\sigma/s$ and $LOQ = 10\sigma/s$ were used to calculate LOD and LOQ. In the aforementioned equations, σ is the standard deviation and S is the slope of the regression line. LOD and LOQ of naproxen incorporated in above equations were determined as 1.87×10^{-4} mol/L and 5.64×10^{-4} mol/L, respectively. The relative error of current method (1%) was obtained which is lower than the values reported in the literature, 1.4% [15] and 3.5% [28] and similar to 1% [32]. Based on obtained results, the method developed in this study is quite reliable. Table 2 summarized the comparative analyses for the detection of S-naproxen by HPLC and spectroscopy methods. This table reveals the rate of relative error and linear coefficient of analysis of S-naproxen determination in naproxen tablets with the developed method compared to the methods that determining naproxen. The rate of the relative error in the analysis of determining S-naproxen in the present naproxen samples with the developed method indicates the accuracy and precision of the present method. In comparison with other methods, the accuracy of the method developed in the analysis of determining S-naproxen in naproxen samples indicates the efficiency of that method in diagnosis.

The relative error and linear coefficient of present method were 1% and 0.993, respectively. A quick and inexpensive analytical approach for naproxen determining separates the current method from HPLC. As well, the present method detected naproxen with a lower relative error compared to similar methods. The changes in the linear dynamic range, accuracy, and analysis of determining S-naproxen in naproxen drug samples developed by

Table 1. Determination of naproxen using proposed method.

Method	Naproxen ($\mu\text{g mL}^{-1}$)	Found ($\mu\text{g mL}^{-1}$)	Recovery (%)
Spectroscopy	100	99.60	99.670
Spectroscopy	120	119.37	99.475
	140	138.43	98.878
	160	158.57	99.106

Table 2. Comparison of the results of naproxen detection using various methods.

Method	R ²	RE (%)	Ref.
HPLC	0.999	–	[31]
Spectroscopy	0.998	3.5	[28]
	0.999	1.4	[15]
	0.995	1	[32]
	0.993	1	This work

this method indicate that the cultivars are well comparable to many of the reported methods for determining naproxen (Table 2).

4. Conclusion

Holistically, Ag@ Alg core–shell NPs were in-situ synthesized and characterized using various analytical methods. Based on obtained results, Ag@ Alg NPs possess a crystalline structure with uniform size distribution. Ag@ Alg NPs presented potential application in the detection of S-naproxen drug in pharmaceutical formulations. The capability of the Ag@ Alg NPs in the detection of S-naproxen was evaluated under different pH values and reaction time. According to the findings of this research, the produced core–shell nanostructure can detect S-naproxen in near-alkaline settings with a relative error of 1% when assessing naproxen concentration. With the use of UV–Vis spectrophotometry, which is a quick and affordable analytical technique, this research could successfully present effort created a novel detection approach for chiral pharmaceuticals. The findings this study suggest that naproxen dosage detection in blood serum during clinical trials and quality control testing in the naproxen pharmaceutical industry may both be accomplished using silver nanoparticles with an alginate coating. The stability of the synthesized materials is durable and does not lose its properties under normal temperature conditions which is biodegradable and non-toxic.

Conflicts of interest

The authors declare that they have no competing interests.

Acknowledgment

We would like to appreciate the support of the Department of Chemical Engineering at the Faculty of Engineering, Central Tehran Branch Islamic Azad University, and Professor Najafpour's Biotechnology Laboratory at Noshirvan University of Technology, Iran, for this research.

References

- [1] Y. Li, L. Gang, W. Li, F. Yang, H. Liu, Greenly Synthesized Gold-Alginate Nanocomposites Catalyst for Reducing Decoloration of Azo-Dyes, *Nano* 10 (2015) 1–10, <https://doi.org/10.1142/S1793292015501088>.
- [2] Y. Sun, Z. Zhang, Z. Xi, Z. Shi, Determination of naproxen in human urine by high-performance liquid chromatography with direct electrogenerated chemiluminescence detection, *Talanta* 79 (2009) 676–680, <https://doi.org/10.1016/j.talanta.2009.04.048>.
- [3] Y. Liu, Y. Liu, Z. Liu, X. Zhao, J. Wei, H. Liu, X. Si, Z. Xu, Z. Cai, Chiral molecularly imprinted polymeric stir bar sorptive extraction for naproxen enantiomer detection in PPCPs, *J. Hazard. Mater.* 392 (2020) 122251, <https://doi.org/10.1016/j.jhazmat.2020.122251>.
- [4] S. Mehta, A.K. Sharma, R. Singh, Development and validation of HPTLC method for simultaneous estimation of bioactive components in combined extracts of three hepatoprotective plants, *J. Liq. Chromatogr.* 44 (2021) 375–381, <https://doi.org/10.1080/10826076.2021.1939046>.
- [5] M.R. Siddiqui, Z.A. AlOthman, N. Rahman, Analytical techniques in pharmaceutical analysis: a review, *Arab. J. Chem.* 10 (2017) 1409–1421, <https://doi.org/10.1016/j.arabjc.2013.04.016>.
- [6] M. Jafari, J. Tashkhourian, G. Absalan, Chiral recognition of tryptophan enantiomers using chitosan-capped silver nanoparticles: scanometry and spectrophotometry approaches, *Talanta* 178 (2018) 870–878, <https://doi.org/10.1016/j.talanta.2017.10.005>.
- [7] M. Ahmadi, T. Madrakian, A. Afkhami, Enantioselective solid phase extraction prior to spectrofluorometric determination: a procedure for the determination of naproxen enantiomers in the presence of each other, *RSC Adv.* 5 (2015) 5450–5457, <https://doi.org/10.1039/C4RA10405F>.
- [8] A. Mohammed Alrashidy, K. Badrany, G. Garagoly, Spectrophotometric determination of sulphamethoxazole drug by new pyrazoline derived from 2,4-dinitro phenyl hydrazine, *Mater. Sci. Forum.* 1002 (2020) 350–359, <https://doi.org/10.4028/www.scientific.net/MSF.1002.350>.
- [9] B. Joda, Z. Al-Kadhim, H. Ahmed, A. Al-Khalaf, A Convenient green method to synthesize β -carotene from edible carrot and nanoparticle formation, *Karbala Int. J. Mod. Sci.* 8 (2022) 1–8, <https://doi.org/10.33640/2405-609X.3200>.
- [10] M.R. Eslami, N. Alizadeh, Nanostructured conducting molecularly imprinted polypyrrole based quartz crystal microbalance sensor for naproxen determination and its electrochemical impedance study, *RSC Adv.* 6 (2016) 9387–9395, <https://doi.org/10.1039/C5RA21489K>.
- [11] A. Nina, K. Fereshteh, Simple, sensitive and selective spectrophotometric assay of naproxen in pure, pharmaceutical preparation and human serum samples, *Acta Pol. Pharmaceut. Drug Res.* 72 (2015) 867–875, <https://doi.org/10.5267/J.CCL.2013.10.006>.
- [12] N. Akhlaghi, G. Najafpour-Darzi, Multifunctional metal-chelated phosphonate/Fe₃O₄ magnetic nanocomposite particles for defeating antibiotic-resistant bacteria, *Powder Technol.* 384 (2021) 1–8, <https://doi.org/10.1016/j.powtec.2021.01.078>.
- [13] R. Esmail, A. Afshar, M. Morteza, A. Abolfazl, E. Akhondi, Synthesis of silver nanoparticles with high efficiency and stability by culture supernatant of *Bacillus ROM6* isolated from Zarshouran gold mine and evaluating its antibacterial effects, *BMC Microbiol.* 22 (2022) 87–97, <https://doi.org/10.1186/s12866-022-02490-5>.
- [14] J. Tashkhourian, M. Afsharinejad, A.R. Zolghadr, Colorimetric chiral discrimination and determination of S-citalopram based on induced aggregation of gold nanoparticles, *Sens. Actuator B Chem.* 232 (2016) 52–59, <https://doi.org/10.1016/j.snb.2016.03.097>.
- [15] J. Tashkhourian, M. Afsharinejad, Chiral recognition of naproxen enantiomers using starch capped silver nanoparticles, *Anal. Methods* 8 (2016) 2251–2258, <https://doi.org/10.1039/C5AY03021H>.
- [16] D. Dawood Ali Salim, L.S. Chua, T.S. Tan, A.F. Alshemary, Biosynthesis, characterization and antiproliferative activity of green synthesized gold nanoparticles using Lantana-dene A extracted from *Lantana camara*, *Karbala Int. J. Mod. Sci.* 7 (2021) 313–326, <https://doi.org/10.33640/2405-609X.3158>.
- [17] E.A. Terenteva, V.V. Apyari, E.V. Kochuk, S.G. Dmitrienko, Y.A. Zolotov, Use of silver nanoparticles in spectrophotometry, *J. Anal. Chem.* 7 (2017) 1138–1154, <https://doi.org/10.1134/S1061934817110107>.
- [18] V.V. Apyari, E.A. Terenteva, A.R. Kolomnikova, A.V. Garshev, S.G. Dmitrienko, Y.A. Zolotov, Potentialities of Differently-Stabilized Silver Nanoparticles for Spectrophotometric Determination of Peroxides, *Talanta* 202 (2019) 51–58, <https://doi.org/10.1016/j.talanta.2019.04.056>.
- [19] S. Beisl, S. Monteiro, R. Santos, A.S. Figueiredo, M.G. Sánchez-Loredo, M.A. Lemos, F. Lemos, M. Minhalma, M.N. de Pinho, Synthesis and bactericidal activity of nanofiltration composite membranes – cellulose acetate/silver nanoparticles and cellulose acetate/silver ion exchanged zeolites, *Water Res.* 149 (2019) 225–231, <https://doi.org/10.1016/j.watres.2018.10.096>.
- [20] V. Thangaraj, S. Mahmud, W. Li, F. Yang, H. Liu, Greenly synthesised silver-alginate nanocomposites for degrading dyes and bacteria, *IET Nanobiotechnol.* 12 (2018) 47–51, <https://doi.org/10.1049/iet-nbt.2017.0074>.
- [21] F. Saira, H. Razzaq, M. Mumtaz, S. Ahmad, M.A. Rafiq, Y. Yaqub, N. Dilshad, A. Ihsan, M. Masood ul Hasan, Investigation of glucose oxidation at gold nanoparticles deposited at carbon nanotubes modified glassy carbon electrode by theoretical and experimental methods, *Karbala Int. J. Mod. Sci.* 6 (2020) 69–77, <https://doi.org/10.33640/2405-609X.1370>.
- [22] S.K. Sen, T.C. Paul, S. Dutta, M.N. Hossain, M.N.H. Mia, XRD peak profile and optical properties analysis of Ag-doped h-MoO₃ nanorods synthesized via hydrothermal method, *J. Mater. Sci. Mater. Electron.* 31 (2020) 1768–1786, <https://doi.org/10.1007/s10854-019-02694-y>.
- [23] F. Gö, A. Aygün, A. Seyrankaya, T. Gür, C. Yenikaya, F. Şen, Green synthesis and characterization of *Camellia sinensis* mediated silver nanoparticles for antibacterial ceramic applications, *Mater. Chem. Phys.* 250 (2020) 1–11, <https://doi.org/10.1016/j.matchemphys.2020.123037>.
- [24] M. Faried, K. Shamel, M. Miyake, A. Hajalilou, A. Zamanian, Z. Zakaria, E. Abouzari-lotf, H. Hara, N.B.B. Ahmad Khairudin, M.F. Binti Mad Nordin, A Green approach for the synthesis of silver nanoparticles using ultrasonic radiation's times in sodium alginate media: characterization and antibacterial evaluation, *J. Nanomater.* 1155 (2016) 1–11, <https://doi.org/10.1155/2016/4941231>.
- [25] H. Zhang, A.M. Omer, Z. Hu, L.-Y. Yang, C. Ji, X.-k. Ouyang, Fabrication of magnetic bentonite/carboxymethyl chitosan/sodium alginate hydrogel beads for Cu (II) adsorption, *Int. J. Biol. Macromol.* 135 (2019) 490–500, <https://doi.org/10.1016/j.jbiomac.2019.05.185>.
- [26] S. Bhagyaraj, I. Krupa, Alginate-Mediated synthesis of hetero-shaped silver nanoparticles and their hydrogen peroxide sensing ability, *Molecules* 25 (2020) 435–447, <https://doi.org/10.3390/molecules25030435>.
- [27] M. Omar, A. Abdelghany, A. Oraby, Optical and dielectric characteristics of polyethylene oxide/sodium alginate-modified gold nanocomposites, *RSC Adv.* 10 (2020) 37621–37630, <https://doi.org/10.1039/D0RA07601E>.
- [28] G. Clua-Palau, E. Jo, S. Nikolic, J. Coello, S. Maspocho, Finding a reliable limit of detection in the NIR determination of residual moisture in a freeze-dried drug product, *J. Pharm. Biomed.* 183 (2020) 113163, <https://doi.org/10.1016/j.jpba.2020.113163>.
- [29] J. Uhrovčík, Strategy for determination of LOD and LOQ values – some basic aspects, *Talanta* 119 (2014) 178–180, <https://doi.org/10.1016/j.talanta.2013.10.061>.

- [30] K. Zhang, Z. Yuan, L. Li, X. Shi, L. Cao, Y. Du, N. Xue, Separation of the two enantiomers of naproxinod by chiral normal-phase liquid chromatography, *J. Chromatogr. Sci.* (2011) 272–275, <https://doi.org/10.1093/chrsi/49.4.272>.
- [31] G. Absalan, Y. Alipour, Z. Rezaei, M. Akhond, Determination of enantiomer compositions of propranolol enantiomers by chiral ionic liquid as a chiral selector and the UV-assisted spectrophotometric method, *Anal. Methods* 4 (2012) 2283–2287, <https://doi.org/10.1039/C2AY25161B>.
- [32] A. Barazandeh, G. Najafpour, A. Alihosseini, S. Kazemi, Spectrophotometric Determination of Naproxen Using Chitosan Capped Silver Nanoparticles in Pharmaceutical Formulation, 2021, pp. 1576–1585, <https://doi.org/10.5829/ije.2021.34.07a.03>.